IFSCC 2025 full paper (IFSCC2025-843)

"Innovative self-assembly technology: a supramolecular ruddy complexion microcapsule with high efficiency for eliminating yellow and whitening"

Hao Li[1] , Xinhang Li[1] , Li Huang[1] , Bo Yang[2] , Mingqing Zhou[2] , Bo Ruan[2] , Zhenyuan Wang[2] , Jiaheng Zhang[3]

[1] **Zhejiang EastGarden Beauty Group Co., Ltd., Hangzhou**; [2] **Shenzhen Shinehigh Innovation Technology Co., Ltd.**; [3] **Harbin Institute of Technology (Shenzhen), Shenzhen , Shenzhen, China**

1. Introduction

The global cosmetics market has experienced a paradigm shift toward products that address eliminating yellow and whitening and the restoration of skin ' s physiological homeostasis. Environmental stressors such as UV light and pollution, combined with intrinsic factors such as oxidative stress and glycation, contribute to dullness, hyperpigmentation and accelerated aging, driving demand for solutions that transcend superficial enhancement [1, 2]. Concurrently, plant active ingredients (e,g, Glycyrrhiza glabra, Paeonia lactiflora, and Angelica sinensis) with antioxidant and cosmetic properties have gained attention for their ability to inhibit melanogenesis, remove free radicals, and stimulate collagen synthesis [3-9]. However, the clinical translation of these phytochemicals is limited by poor bioavailability and instability in conventional formulations, which require advanced delivery systems [10].

Recent advances in deep eutectic solvents (DES) and nanotechnology have revolutionized the delivery of bioactive compounds. The DES, which is composed of hydrogen bond donors (e.g. glycerol) and acceptors (e.g. choline chloride) of hydrophobic phytochemicals, has a higher solubility capacity and is therefore suitable for sensitive skin [11, 12, 13, 14]. For instance, DES-based systems enhance the solubility of curcumin by 12-fold compared to traditional solvents [15]. Meanwhile, nanotechnologies such as nanostructured lipid carriers (NLCs) and polymeric micelles, significantly improve dermal penetration and prolong active retention [16-21]. Nanoparticles show higher transport efficiency and superior safety [22, 23]. Thus, the synergy of DES and nanotechnology provides a superior solution for the development of functional skincare systems [24-26].

The study developed Supra-QSD, a supramolecular, cosmetic microcapsule, by a synergistic combination of deep eutectic solvents (DES) and nanoencapsulation technologies. The plant active ingredients and DES was successfully encapsulated in submicron carriers (180 nm) by ultra-high pressure homogenization, resulting in a 95% of the active substance at 25℃ / 3months, a 2.16 times deeper penetration than oil-based formats, elevated inhibition of AGEs and DPPH radical scavenging.

2. Materials and Methods

2.1 Materials and reagents

Pterocarpus marsupium bark extract (The main ingredient is pterostilbene), and plant extract complexes (replace with QSD) are provided by Zhejiang University of Technology. DES components (bisabolol, 4-t-butylcyclohexanol) and encapsulation materials (caprylic/capric triglyceride, tocopheryl acetate, nonapeptide-1, glycerin, phospholipids, polyglyceryl-10 oleate, polyglyceryl-3 beeswax) were purchased from Sigma-Aldrich.

2.2 Preparation of DES and supramolecular ruddy complexion microcapsule

All preparations were performed under a nitrogen atmosphere to prevent oxidation. Initially, the DES was pre-synthesized by stirring bisabolol and 4-t-butylcyclohexanol at a molar ratio of 2:1 under 50 ± 10℃ and 200–300 rpm for 1 hour to ensure a complete reaction.

Subsequently, the oil phase and aqueous phase were separately homogenized at 70 ± 10℃. The oil phase contains 8% pterocarpus marsupium bark extract, 5% QSD (Contains 0.1% astragalus membranaceus root extract, 0.03% polygonatum officinale rhizome/root extract, 0.15% ganoderma lucidum (mushroom) extract, 0.15% paeonia lactiflora extract, 0.0625% lilium candidum extract, 0.00002% lysimachia christinae extract, 0.0875% rehmannia chinensis root extract), 0.5% DES, 19.41998% caprylic/capric triglyceride, 0.1% tocopheryl acetate, 3% phospholipids and 1.0% polyglyceryl-3 beeswax. The water phase contains 0.05% nonapeptide-1, 15% glycerin, 6% polyglyceryl-10 oleate, and the remaining volume was adjusted with water. The oil phase was slowly added to the aqueous phase under shear dispersion to ensure homogeneity, followed by high-pressure homogenization for four cycles and subsequent cooling, resulting in the supramolecular ruddy complexion microcapsule (Supra-QSD). QSD oil was used as a control containing only the same plant extract complexes and the remaining amount of caprylic/capric triglyceride.

2.3 Vesicle Size, Size Distribution, and Zeta Potential.

The average particle size, polydispersity index (PDI), and zeta potential of nanoparticles were analyzed by dynamic light scattering (DLS) (ZetaLitesizer 500, Anton Paar GmbH, Austria). Measurements were conducted at 25 ± 0.1℃ with a scattering angle of 173° and a laser wavelength of 633 nm.

2.4 Particle Size and Content Stability

To evaluate stability, Samples were aliquoted to be stored under various conditions (25℃, -15℃, 5℃, 45℃, and light exposure) for 3 months. Samples were collected at day 0, day 14, and monthly intervals for particle size and content stability analysis. Particle size was determined by DLS, and content stability was assessed by quantifying pterostilbene recovery rates via high-performance liquid chromatography (HPLC) (Agilent1260, California, CA, USA).

2.5 In vitro transdermal permeation

Transdermal permeation was evaluated using Franz diffusion cytometer (ZX/TP-6, Beijing, China) with pig skin. After incubation for 2h, 4h, and 6h, skin samples were fixed in 4% paraformaldehyde for 4h, sectioned uniformly using a cryostat, and examined by confocal laser scanning microscopy to determine fluorescence distribution and intensity.

2.6 AGEs Inhibition Assay

Anti-glycation activity was evaluated by measuring AGEs inhibition. Test samples were mixed with BSA-fructose solution, while controls included: (1) PBS mixed with BSA-fructose (control), (2) PBS alone (blank control), and (3) sample mixed with PBS (blank sample). After thorough mixing, solutions were incubated at 37°C for 7 days. Absorbance at 517 nm was measured using an enzyme-labeled instrument, with aminoguanidinium sulfate as a positive control. The inhibition percentage was calculated using the following formula:

$$Inhibition\ (\%) = \frac{[(ODcontrol - ODblank\ control) - (ODsample - ODblank\ sample)}{(ODcontrol - ODblank\ control)} \times 100\%$$

2.7 DPPH radical scavenging assay

The antioxidant activity of samples was evaluated by measuring DPPH radical scavenging capacity. Test samples were thoroughly mixed with DPPH solution, while control groups included: (1) absolute ethanol mixed with DPPH solution (control), (2) absolute ethanol alone (blank control), and (3) sample mixed with absolute ethanol (blank sample). After 30 minutes of reaction at room temperature under light-protected conditions, absorbance at 517 nm was measured using an enzyme-labeled instrument. Vitamin C was used as a positive control. The radical scavenging rate was calculated according to the following formula:

$$Inhibition\ (\%) = \frac{[(ODcontrol - ODblank\ control) - (ODsample - ODblank\ sample\ )}{(ODcontrol - ODblank\ control)} \times 100\%$$

2.8 Cell Culture

The human immortalized keratinocyte cell line (HaCaT) was purchased from the American Type Culture Collection (ATCC). Cells were grown in DMEM medium supplemented with 10% fetal bovine serum (FBS), 100 IU/mL penicillin, and 100 μg/mL streptomycin and maintained in a humidified incubator containing 5% CO_2 at 37°C.

2.9 Cellular photodamage protection test

The photodamage repair efficacy was evaluated by assessing the effect of test samples on cell viability following UVB-induced damage. The experimental procedure was as follows: HaCaT cells were seeded in 96-well plates at a density of 2×10^4 cells/well and cultured overnight at 37°C with 5% CO_2. When cells reached approximately 70% confluency, the medium was aspirated and replaced with 100 μL PBS. The cells were then exposed to UVB radiation (40 mJ/cm^2 cumulative dose) using a photoaging simulator. At the same time, an unirradiated blank control was set up. Post-irradiation, the following treatments were applied; Blank control: fresh medium only; Model group: fresh medium; Test groups: drug-containing medium. After 24 hours of additional incubation, the plates were removed and equilibrated at room temperature for 10 minutes. Cell viability was assessed using CCK-8 reagent (10 μL/well) with 1-hour incubation at 37℃. Absorbance was measured at 450 nm (with 600 nm as a reference wavelength). The cell viability percentage was calculated as:

$$Cell\ viability\ (\%) = \frac{ODsample}{ODblank\ control} \times 100\%$$

2.10. Statistical analysis

The mean values (Mean) and standard deviations (SD) were calculated for each experimental group. Statistical analysis was performed using GraphPad Prism software.

Significance levels were defined as follows: $p < 0.05$: statistically significant, $p < 0.01$: highly significant, $p < 0.001$: extremely significant, and $p > 0.05$: not statistically significant.

3. Results and Discussion

3.1 Vesicle Size, Size Distribution, and Zeta Potential.

Particle size and zeta potential critically govern the stability of emulsion systems. Studies indicate that a uniform particle size distribution helps reduce aggregation tendencies, thereby enhancing system stability. Moreover, a higher absolute zeta potential (typically > ±30 mV) strengthens electrostatic repulsion between particles, effectively counteracting van der Waals force-induced aggregation. Conversely, a decrease in zeta potential weakens this repulsion, leading to particle agglomeration and reduced stability [27].

The Supra-QSD exhibited a particle size of 180 nm (PDI = 0.192) (Figure 1 a) and a zeta potential of -41.3 mV (Figure 1 b). Smaller particle size and lower PDI (polydispersity index) indicate a larger comparative surface area among particles, suggesting more complete and efficient encapsulation by the emulsion. Furthermore, an absolute zeta potential exceeding 30 mV demonstrates strong interparticle repulsion, effectively preventing aggregation and subsequent sedimentation due to particle growth. Thus, both particle size and zeta potential data confirm that the Supra-QSD system exhibits excellent stability and dispersibility.

3.2 Particle Size and Content Stability

The long-term variation in particle size demonstrates the Brownian motion of the emulsion during storage while ripening under different conditions indicates its storage stability over the shelf life. Changes in active ingredient content at different time points also reflect the stability of the emulsion system [28].

Monitoring of the samples under various storage conditions for three months demonstrated excellent stability in both particle size and active ingredient content. The samples maintained consistent particle sizes within the range of 170-200 nm across all test conditions (Figure 1 c). Therefore, the minimal change in particle size indicates that Brownian motion did not induce particle aggregation in the system, and the ripening process of the emulsion did not compromise particle stability. In low-temperature storage (5℃ and -15℃), active ingredient recovery rates remained >98% after 3 months (Figure 1 d). In room temperature (25℃), active ingredient recovery rates remained >95% after 3 months (Figure 1 d). Though slightly reduced stability was observed after 3 months in stress condition (45℃), recovery rates remained at ~90% (Figure 1 d). Therefore, the minimal change in particle size indicates that Brownian motion did not induce particle aggregation in the system, and the ripening process of the emulsion did not compromise particle stability.

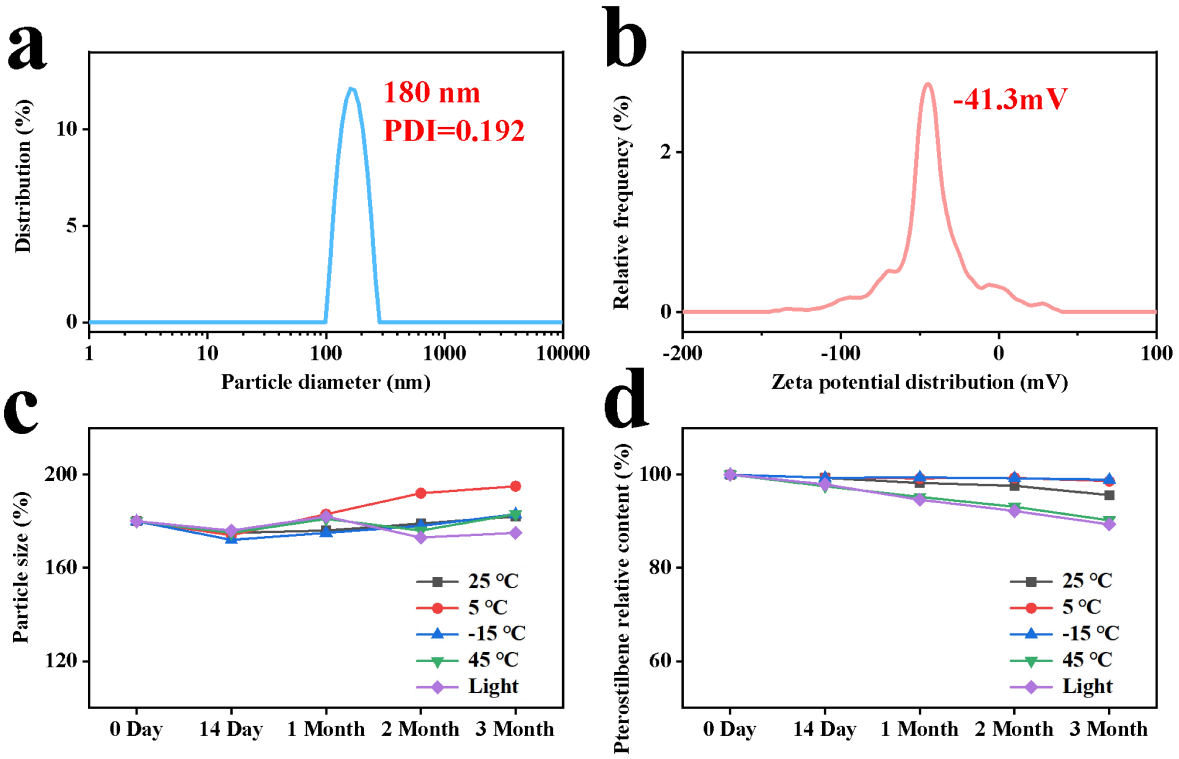

Figure 1. Characterisations of Supra-QSD (a) Particle size distribution, (b) Zeta potential distribution, (c) Particle size stability, (d) Content stability

3.3 In vitro transdermal permeation

Transdermal delivery in cosmetics involves the permeation of actives through the skin barrier to reach target layers (e.g., stratum corneum, epidermis, or dermis), directly influencing product efficacy. Permeation pathways include intercellular lipid diffusion, intracellular penetration, or transport via skin appendages such as hair follicles and sweat glands [29]. Optimized transdermal delivery enhances the bioavailability of functional ingredients (e.g., whitening or anti-aging agents), while modern technologies such as targeted delivery and sustained-release systems penetration depth with safety to ensure synergistic optimization of efficacy and skin health [30].

Confocal laser scanning microscopy (CLSM) analysis revealed the dermal penetration efficacy of the Supra-QSD. The active components were observed to progressively migrate from the stratum corneum through the epidermis, ultimately reaching the dermal layer (Figure 2). Supra-QSD demonstrates time-dependent transdermal accumulation. Fluorescence intensity analysis further corroborated these findings, showing a 2.16-fold enhancement relative to the oil formulation (Figure 3 a). These results demonstrate that supramolecular microencapsulation markedly improves percutaneous penetration, thereby optimizing the bioavailability of active ingredients. This depth-resolved penetration behavior confirms the enhanced transdermal delivery capability achieved through supramolecular modification.

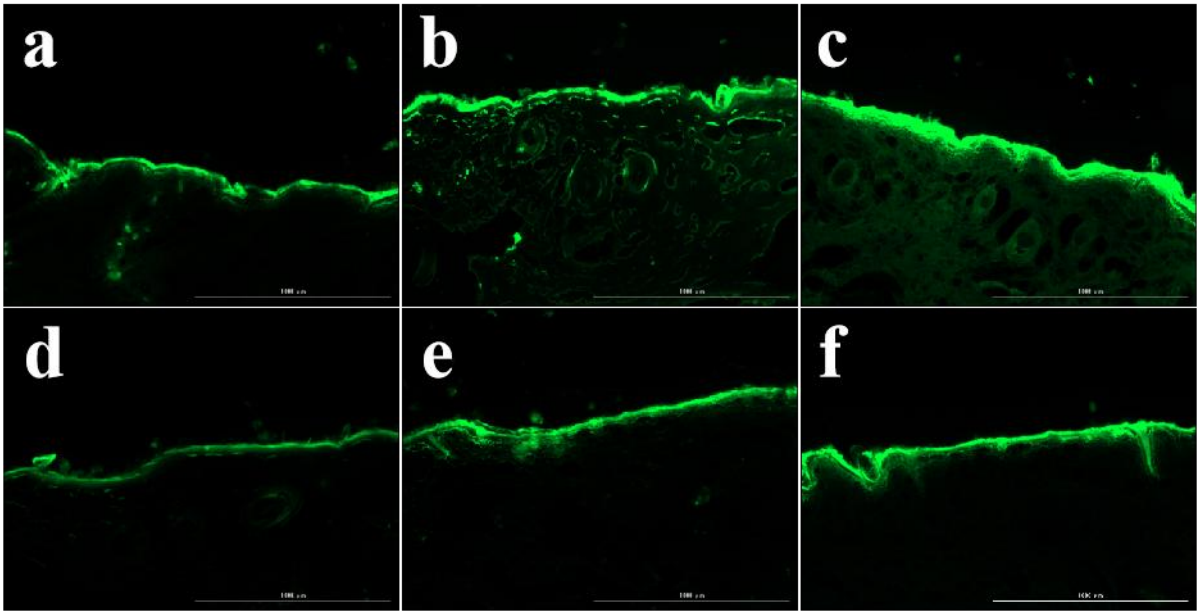

Figure 2. Dermal penetration efficacy of Supra-QSD versus QSD oil. (a) (b) (c) Fluorescence dermal penetration images of Supra-QSD at 2, 4 and 6 hours, respectively. (d) (e) (f) Fluorescence dermal penetration images of QSD oil at 2, 4 and 6 hours, respectively.

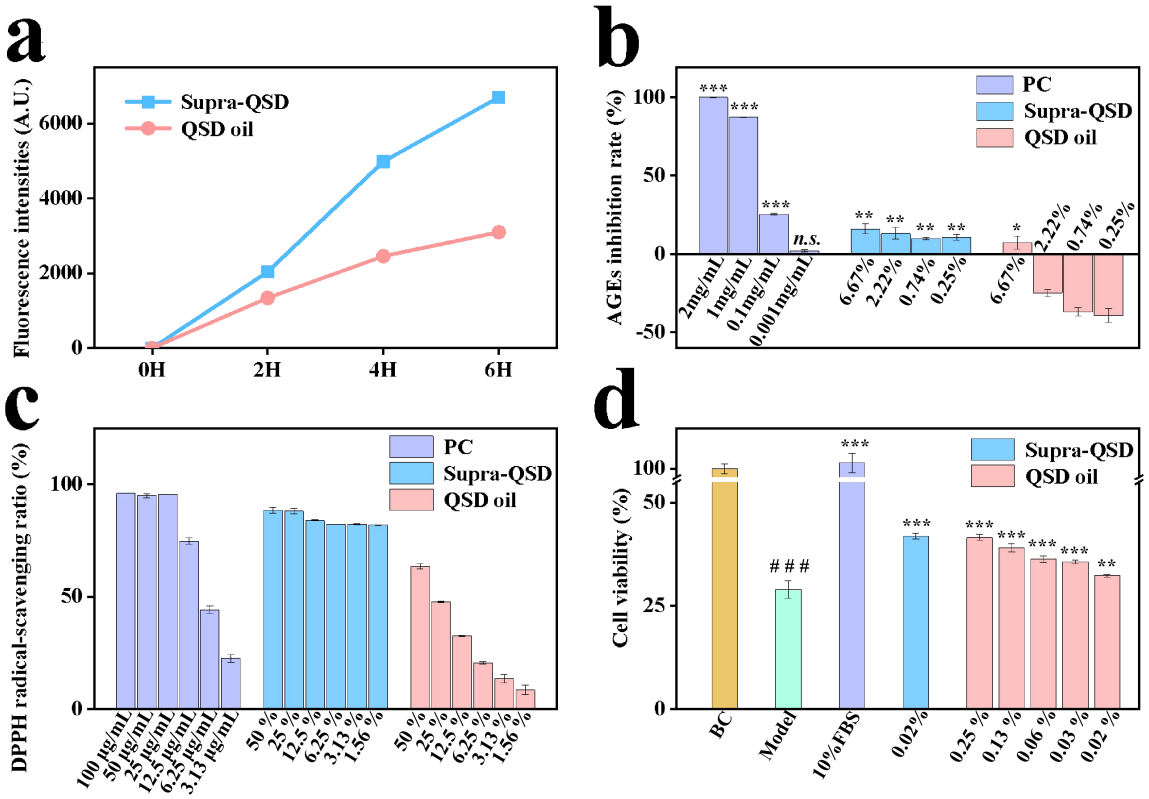

Figure 3. Efficacy Analysis (a) Transdermal fluorescence intensity. (b) AGEs inhibition rates. PC: Aminoguanidine Hemisulfate; ***p < 0.001, **p < 0.01, *p < 0.05, n.s. p < 0.05 vs. blank control. (c) DPPH radical scavenging capacity, PC: Vitamin C. (d) UVB photoprotection assay. Viability measured by CCK-8 assay; BC: Blank control; Model: UVB model; ###p < 0.001 model vs. control; ***p<0.001,**p<0.01,*p<0.05 vs. model."

3.4 AGEs inhibition

Advanced Glycation End Products (AGEs) serve as critical biomarkers for evaluating the anti-glycation efficacy of active compounds. Their formation involves non-enzymatic reactions between reducing sugars with proteins, lipids and/or nucleic acids ultimately leading to protein cross-linking, functional impairment, and tissue damage. Quantitative analysis of AGEs and their intermediates provides a reliable framework for the systematic assessment of the anti-glycation potential of bioactive ingredients [31].

The inclusion of a positive control confirmed the efficacy of the experimental system, with a statistically significant difference observed compared to the blank control ($p < 0.05$). The Supra-QSD demonstrated significant dose-dependent inhibition of AGEs formation, exhibiting superior efficacy to conventional QSD oil formulations at equivalent concentrations (Figure 3 b). Notably, while the QSD oil only showed detectable inhibition at high concentrations (6.67%), the Supra-QSD maintained significant anti-glycation activity even at lower doses, outperforming the highly concentrated QSD oil solution. These results indicate that the supramolecular modification confers enhanced anti-glycation properties to the QSD active.

3.5 DPPH free radical scavenging

Free radical-mediated processes represent a critical focus in skin research due to their involvement in diverse dermatological conditions, including skin cancer, photoaging, and intrinsic aging [32]. Upon UV exposure, reactive oxygen species (ROS) and free radicals cause peroxidative damage to cell membranes, ultimately leading to irreversible cellular dysfunction [33].

As shown in Figure 3 c, the Supra-QSD exhibited dose-dependent antioxidant activity, with significantly greater DPPH radical scavenging efficiency compared to conventional QSD oil at equivalent concentrations. Notably, the supramolecular formulation achieved near-equivalent antioxidant efficacy to positive control (vitamin C) at matched doses, while maintaining superior performance at lower concentrations. These results demonstrate that the supramolecular modification confers potent free radical-neutralizing capability to the QSD active.

3.6 Cellular photodamage protection

UVB exposure to radiation induces the accumulation of large amounts of ROS in the skin and induces skin-associated cellular dysfunction with a variety of negative effects, including increased inflammation and extracellular matrix degradation [34]. Suppression of UVB radiation-induced photodamage to the skin cells is important for skin health. The Supra-QSD demonstrated significant protective effects against UVB-induced damage in HaCaT keratinocytes, outperforming the conventional QSD oil formulation at equivalent concentrations (Figure 3 d). UVB irradiation (40 mJ/cm²) significantly reduced cell viability vs. untreated control (###$p < 0.001$), which confirmed the successful induction of the photodamage model. Therefore, Supra-QSD can significantly reduce the photodamaging effects of UVB on HaCaT keratinocytes and have a protective effect on cells.

4. Conclusion

This study successfully developed a Supra-QSD microcapsule system through the innovative integration of plant extract complexes, DES, and nano-encapsulation technologies. Comprehensive characterization demonstrated excellent stability (180 nm particle size with PDI=0.192; >95% active retention at 25°C/3 months) and significantly enhanced transdermal permeation (2.16 times higher than that of QSD oil). The Supra-QSD has demonstrated multifunctional efficacy, including potent anti-glycation, superior antioxidant activity and remarkable photoprotection. These advances are attributed to DES and nanoencapsulation technologies that have led to increased stabilization and bioavailability of actives as well as targeted delivery. The results confirm the superiority of the Supra-QSD as a breakthrough platform that effectively combines traditional plant extracts with modern pharmaceutical science and offers a technologically advanced solution for multifunctional cosmetics. This work not only provides a model for modernizing traditional ingredients but also lays the

ground for the development of next-generation cosmetics with improved stability, delivery and efficacy profiles.

Data Availability

All the relevant data are available from the corresponding authors upon reasonable request.

Declaration of Competing Interests

The authors declare no conflict of interest.

Animal free statement

All sources involved in the study met the requirements. The pig skins used were from pigs slaughtered for food and not pigs slaughtered for experimental purposes.

References

1. Zgutka, K., Tkacz, M., Tomasiak, P., & Tarnowski, M. (2023). A role for advanced glycation end products in molecular ageing. International journal of molecular sciences, 24(12), 9881.
2. Pillaiyar, T., Manickam, M., & Namasivayam, V. (2017). Skin whitening agents: Medicinal chemistry perspective of tyrosinase inhibitors. Journal of enzyme inhibition and medicinal chemistry, 32(1), 403-425.
3. Cerulli, A., Masullo, M., Montoro, P., & Piacente, S. (2022). Licorice (Glycyrrhiza glabra, G. uralensis, and G. inflata) and their constituents as active cosmeceutical ingredients. Cosmetics, 9(1), 7.
4. Hao, L. I. N., Qiyu, C. H. E. N., Zhipeng, L. O. N. G., & Haihong, X. I. A. O. (2024). Antioxidant activity and efficacy evaluation of Angelica sinensis and Peony bark extract. China Food Additives, 35(6), 34.
5. Lee, S. C., Kwon, Y. S., Son, K. H., Kim, H. P., & Heo, M. Y. (2005). Antioxidative constituents from Paeonia lactiflora. Archives of Pharmacal Research, 28, 775-783.
6. Michalak, M. (2023). Plant extracts as skin care and therapeutic agents. International journal of molecular sciences, 24(20), 15444.
7. Campa, M., & Baron, E. (2018). Anti-aging effects of select botanicals: Scientific evidence and current trends. Cosmetics, 5(3), 54.
8. Qiu, J., Chen, M., Liu, J., Huang, X., Chen, J., Zhou, L., ... & Jeulin, S. (2016). The skin‐depigmenting potential of Paeonia lactiflora root extract and paeoniflorin: in vitro evaluation using reconstructed pigmented human epidermis. International Journal of Cosmetic Science, 38(5), 444-451.
9. Chen, Y., Li, H., Zhang, X. L., Wang, W., Rashed, M. M., Duan, H., ... & Zhai, K. F. (2024). Exploring the anti-skin inflammation substances and mechanism of Paeonia lactiflora Pall. Flower via network pharmacology-HPLC integration. Phytomedicine, 129, 155565.
10. Lin, T. K., Zhong, L., & Santiago, J. L. (2018). Anti-inflammatory and skin barrier repair effects of topical application of some plant oils. International journal of molecular sciences, 19(1), 70.
11. Abbott, A. P., Capper, G., Davies, D. L., Rasheed, R. K., & Tambyrajah, V. (2003). Novel solvent properties of choline chloride/urea mixtures. Chemical communications, 9(1), 70-71.
12. Fu, M., Zhang, H., Bai, J., Cui, M., Liu, Z., Kong, X., ... & Kong, L. (2025). Application of Deep Eutectic Solvents with Modern Extraction Techniques for the Recovery of Natural Products: A Review. ACS Food Science & Technology, 5(2), 444–461.

13. Ramon, M. R., Durand, E., Garcia-Sosa, K., & Peña-Rodríguez, L. M. (2023). Exploring the potential of deep eutectic solvents (DES) in bioactive natural product research: from DES to NaDES, THEDES, and beyond. PeerJ Analytical Chemistry, 5, e28.
14. Kumar, A., Saha, M., Vishwakarma, R., Behera, K., & Trivedi, S. (2024). Green solvents tailored nanostructures of block copolymers and their potential applications in drug delivery. Journal of Molecular Liquids, 410, 125642.
15. Duarte, A. R. C., Ferreira, A. S. D., Barreiros, S., Cabrita, E., Reis, R. L., & Paiva, A. (2017). A comparison between pure active pharmaceutical ingredients and therapeutic deep eutectic solvents: Solubility and permeability studies. European Journal of Pharmaceutics and Biopharmaceutics, 114, 296-304.
16. Patil, T. S., Gujarathi, N. A., Aher, A. A., Pachpande, H. E., Sharma, C., Ojha, S., ... & Agrawal, Y. O. (2023). Recent advancements in topical anti-psoriatic nanostructured lipid carrier-based drug delivery. International journal of molecular sciences, 24(3), 2978.
17. Stefanov, S. R., & Andonova, V. Y. (2021). Lipid nanoparticulate drug delivery systems: recent advances in the treatment of skin disorders. Pharmaceuticals, 14(11), 1083.
18. Gugleva, V., Ivanova, N., Sotirova, Y., & Andonova, V. (2021). Dermal drug delivery of phytochemicals with phenolic structure via lipid-based nanotechnologies. Pharmaceuticals, 14(9), 837.
19. Peng, S., Li, Z., Zou, L., Liu, W., Liu, C., & McClements, D. J. (2018). Enhancement of curcumin bioavailability by encapsulation in sophorolipid-coated nanoparticles: an in vitro and in vivo study. Journal of agricultural and food chemistry, 66(6), 1488-1497.
20. Müller, R. H., & Runge, S. A. (2019). Solid lipid nanoparticles (SLN®) for controlled drug delivery. In Submicron emulsions in drug targeting and delivery (pp. 219-234). CRC Press.
21. Chen, S. (2025). Advancement in Nanocarrier-Based Whitening Cosmetics: Mechanisms, Applications, and Future Prospects. Advances in Engineering Technology Research, 13(1), 1296-1296.
22. Ayumi, N. S., Sahudin, S., Hussain, Z., Hussain, M., & Samah, N. H. A. (2019). Polymeric nanoparticles for topical delivery of alpha and beta arbutin: preparation and characterization. Drug delivery and translational research, 9, 482-496.
23. Peng, X., Ma, Y., Yan, C., Wei, X., Zhang, L., Jiang, H., ... & Gao, Y. (2024). Mechanism, Formulation, and Efficacy Evaluation of Natural Products for Skin Pigmentation Treatment. Pharmaceutics, 16(8), 1022.
24. Li, M., Yuan, J., Liu, Z., Yin, T., & Peng, C. (2024). Multifunctional deep eutectic solvent-based microemulsion for transdermal delivery of artemisinin. Langmuir, 40(10), 5098-5105.
25. Zhang, Y., Cao, Y., Meng, X., Li, C., Wang, H., & Zhang, S. (2020). Enhancement of transdermal delivery of artemisinin using microemulsion vehicle based on ionic liquid and lidocaine ibuprofen. Colloids and Surfaces B: Biointerfaces, 189, 110886.
26. Yusakul, G., Chunglok, W., Warinhomhoun, S., & Plyduang, T. (2024). Solubility and stability of curcuminoids in microemulsions formulated with hydrophobic and hydrophilic deep eutectic solvents and their in vitro anti-inflammatory effects. Journal of Drug Delivery Science and Technology, 101, 106272.
27. Niu Hui, Wang Wenduo, Dou Zuman, Chen Xianwei, Chen Xianxiang, Chen Haiming, ... & Fu Xiong. (2023). Multiscale combined techniques for evaluating emulsion stability: A critical review. Advances in Colloid and Interface Science, 311, 102813.
28. Müller, F. K., & Costa, F. F. (2024). Innovations and stability challenges in food emulsions. Sustainable Food Technology.3, 96-122.
29. Kalia, Y. N., & Guy, R. H. (2001). Modeling transdermal drug release. Advanced drug

delivery reviews, 48(2-3), 159-172.
30. Paudel, K. S., Milewski, M., Swadley, C. L., Brogden, N. K., Ghosh, P., & Stinchcomb, A. L. (2010). Challenges and opportunities in dermal/transdermal delivery. Therapeutic delivery, 1(1), 109-131.
31. Wang, L., Jiang, Y., & Zhao, C. (2024). The effects of advanced glycation end‐products on skin and potential anti‐glycation strategies. Experimental dermatology, 33(4), e15065.
32. Herrling, T., Jung, K., & Fuchs, J. (2008). The role of melanin as protector against free radicals in skin and its role as free radical indicator in hair. Spectrochimica Acta Part A: Molecular and Biomolecular Spectroscopy, 69(5), 1429-1435.
33. Lalhminghlui, K., & Jagetia, G. C. (2018). Evaluation of the free-radical scavenging and antioxidant activities of Chilauni, Schima wallichii Korth in vitro. Future science OA, 4(2), FSO272.
34. Chen, B., Yu, L., Wu, J., Qiao, K., Cui, L., Qu, H., ... & Wang, Q. (2022). Effects of collagen hydrolysate from large hybrid sturgeon on mitigating ultraviolet B-induced photodamage. Frontiers in bioengineering and biotechnology, 10, 908033.